J Biomol NMR (2012) 52:103–114
DOI 10.1007/s10858-011-9586-1

ARTICLE

Biomass production of site selective $^{13}C/^{15}N$ nucleotides using wild type and a transketolase *E. coli* mutant for labeling RNA for high resolution NMR

Chandar S. Thakur · Yiling Luo · Bin Chen · Nadukkudy V. Eldho · T. Kwaku Dayie

Received: 2 November 2011 / Accepted: 6 November 2011 / Published online: 29 November 2011

Abstract Characterization of the structure and dynamics of nucleic acids by NMR benefits significantly from position specifically labeled nucleotides. Here an *E. coli* strain deficient in the transketolase gene (tktA) and grown on glucose that is labeled at different carbon sites is shown to facilitate cost-effective and large scale production of useful nucleotides. These nucleotides are site specifically labeled in C1′ and C5′ with minimal scrambling within the ribose ring. To demonstrate the utility of this labeling approach, the new site-specific labeled and the uniformly labeled nucleotides were used to synthesize a 36-nt RNA containing the catalytically essential domain 5 (D5) of the brown algae group II intron self-splicing ribozyme. The D5 RNA was used in binding and relaxation studies probed by NMR spectroscopy. Key nucleotides in the D5 RNA that are implicated in binding Mg^{2+} ions are well resolved. As a result, spectra obtained using selectively labeled nucleotides have higher signal-to-noise ratio compared to those obtained using uniformly labeled nucleotides. Thus, compared to the uniformly $^{13}C/^{15}N$-labeled nucleotides, these specifically labeled nucleotides eliminate the extensive ^{13}C–^{13}C coupling within the nitrogenous base and ribose ring, give rise to less crowded and more resolved NMR spectra, and accurate relaxation rates without the need for constant-time or band-selective decoupled NMR experiments. These position selective labeled nucleotides should, therefore, find wide use in NMR analysis of biologically interesting RNA molecules.

Keywords Alternate-site specific labeling · Transketolase mutant · D5 ribozyme RNA · TROSY · Ribose and nucleobase · RNA · Structure and dynamics

Abbreviations

AMP	Adenosine 5′-monophosphate
CMP	Cytidine 5′-monophosphate
UMP	Uridine 5′-monophosphate
GMP	Guanosine 5′-monophosphate
R5P	Ribose-5-phosphate
F6P	Fructose-6-phosphate
GA3P	Glyceraldehyde-3-phosphate
G6PDH	Glucose-6-phosphate dehydrogenase
K10zwf	Glucose-6-phosphate dehydrogenase mutant
Gly	Glycine
Ser	Serine
noPPP	Non-oxidative pentose phosphate pathway
OAA	Oxaloacetate
DHAP	Dihydroxyacetone phosphate
oPPP	Oxidative pentose phosphate pathway
rNTPs	Ribonucleoside triphosphates
TIM	Triosephosphate isomerase
PEP	Phosphoenolpyruvate
G6P	Glucose-6-phosphate
Ru5P	Ribulose-5-phosphate
X5P	Xylulose-5-phosphate
S7P	Sedoheptulose-7-phosphate
E4P	Erythrose-4-phosphate
3PG	3-Phosphoglycerate
tktA	Transketolase

C. S. Thakur · Y. Luo · B. Chen · N. V. Eldho · T. K. Dayie (✉)
Department of Chemistry and Biochemistry, Center for Biomolecular Structure and Organization, University of Maryland, 1115 Biomolecular Sciences Bldg (#296), College Park, MD 20742-3360, USA
e-mail: dayie@umd.edu

Introduction

RNA molecules have taken center stage in effecting a broad range of important biological functions, partly because they can adopt complex three-dimensional (3D) architectures that are pliable and adaptable to their environment (Al-Hashimi and Walter 2008; Dayie 2008; Hall 2008; Lu et al. 2010). The development of isotopic labeling methods in making uniformly labeled RNA (Batey et al. 1992; Nikonowicz et al. 1992; Michnicka et al. 1993; Hines et al. 1994) had an impact on the development of multidimensional NMR techniques to explore the structural characteristics of small to medium sized RNA molecules (Batey et al. 1995; Latham et al. 2005). However, incorporation of site specific isotopically labeled nucleotides into RNA is necessary to overcome the drawbacks of uniform labeling (Johnson et al. 2006; Johnson and Hoogstraten 2008; Schultheisz et al. 2008; Dayie and Thakur 2010; Thakur et al. 2010a, b; Thakur and Dayie 2011) as we and others have demonstrated using RNAs labeled with uniform and selective NTPs (Johnson et al. 2006; Johnson and Hoogstraten 2008; Schultheisz et al. 2008; Dayie and Thakur 2010; Thakur et al. 2010a, b; Thakur and Dayie 2011). Previous work had focused on site specific labeling using the gluconeogenic carbon sources of glycerol, glycerol and formate, pyruvate, or acetate using either wild type or two mutant *E. coli* strains (Hoffman and Holland 1995; Johnson et al. 2006; Johnson and Hoogstraten 2008; Dayie and Thakur 2010; Thakur et al. 2010a, b; Thakur and Dayie 2011), and glucose using wild type *E. coli* (Kishore et al. 2005). However because *E. coli* grows readily on glucose with very good yield compared to the other gluconeogenic carbon precursors (Thakur et al. 2010a), it is attractive to explore glucose as an alternative carbon source. Unfortunately, all the *E. coli* strains used so far have undesirable scrambling in the ribose ring when grown on glucose.

Most of the scrambling in the ribose region is caused by the admixture of the metabolic flux from both the oxidative pentose phosphate pathway (oPPP) and the non-oxidative pentose phosphate pathway (noPPP) (Josephson and Fraenkel 1969; Josephson and Fraenkel 1974). Thus, an *E. coli* variant that had the noPPP genes disabled would provide new labels without the undesired scrambling when grown on glucose (Fig. 1). The transketolase (tktA) enzyme shunts metabolites in both directions of the noPPP. Deletion of this enzyme, therefore, would enable the redirection of most of the metabolic flux through the oPPP (Fig. 1). To test this hypothesis, K-12 *E. coli* strain was grown on labeled [2-^{13}C]-glucose, whereas tktA *E. coli* was grown on either [1-^{13}C]-glucose, or [2-^{13}C]-glucose, or both [1-^{13}C]-glucose and [2-^{13}C]-glucose. To compare to previous work, K12 *E. coli* was also grown on [1-^{13}C]-acetate and [2-^{13}C]-acetate (Thakur and Dayie 2011). The results demonstrate the advantages of the new, site-specifically labeled nucleotides for NMR structural and dynamics studies.

Fig. 1 Metabolic pathway involved in the production of nucleic acid nucleotides from glucose for wild type and tktA *E. coli* strain as derived from Covert and Palsson (2002). Atom labels for the terminal (1, 6) carbons (*magenta* and *thin circle*) and central (2, 5) carbon (*cyan* and *thick circle*) of glucose are highlighted. Positions that are enriched due to the presence of $^{13}CO_2$ in the growth medium are shown with an *X*. Pyrimidine base derived from the oxaloacetate (OAA). The labeling pattern of purines from glycine derived from 3-phosphate glycerate (3PG) are shown such that if [1-^{13}C]-glucose is used only the C^{β} position of Gly and therefore C2 and C8 positions of the purine ring are labeled. Otherwise if [2-^{13}C]-glucose is used the C^{α} of Gly and therefore C5 of the purine ring is labeled. The segments labeled I are the patterns of labeling expected from both oPPP and noPPP, and those labeled II are labeling patterns expected if GA3P is derived from glycolysis. For the TCA cycle, the expected pattern of labeling following the first, second, and fourth passes through the cycle are also shown

Materials and methods

Bacterial strains

The mutant strain tktA (CGSC # 11606, F-, Δ(araD-araB)567, ΔlacZ4787(::rrnB-3), λ^-, ΔtktA783::kan, rph-1, Δ(rhaD-rhaB)568, hsdR514) and the wild-type K12 strain (Clowes 1968) (CGSC # 4401:F$^+$) used in this work were obtained from the Yale Coli Genetic Stock Center; Dr. Paliy kindly provided the wild-type K12 NCM3722 (Soupene et al. 2003).

Isotopes

The following isotopic-enriched compounds were purchased from Cambridge Isotope Laboratory (Andover, MA) and Isotec-Sigma-Aldrich (Miamisburg, OH): [1-^{13}C]-glucose (99%), [2-^{13}C]-glucose (99%), [1-^{13}C]-acetate (99%), [2-^{13}C]-acetate (99%) and [^{15}N]–$(NH_4)_2SO_4$ (99%).

Media for bacterial growth

Both Luria–Bertani (LB) and LeMaster Richard (LMR) minimal media were prepared as described (Sambrook and Russell 2001; Dayie and Thakur 2010; Thakur et al. 2010a, b; Thakur and Dayie 2011). The LMR media contains 176 mM KH_2PO_4, 25 mM NaOH, 10 µl H_2SO_4, 12.6 mM $(NH_4)_2SO_4$, 2 mM $MgSO_4$, 10 µM $FeSO_4$ and 0.2% trace metals, supplemented with the appropriate ^{13}C-enriched carbon (glucose or acetate) and ^{15}N-enriched nitrogen ($(^{15}NH_4)_2SO_4$) sources.

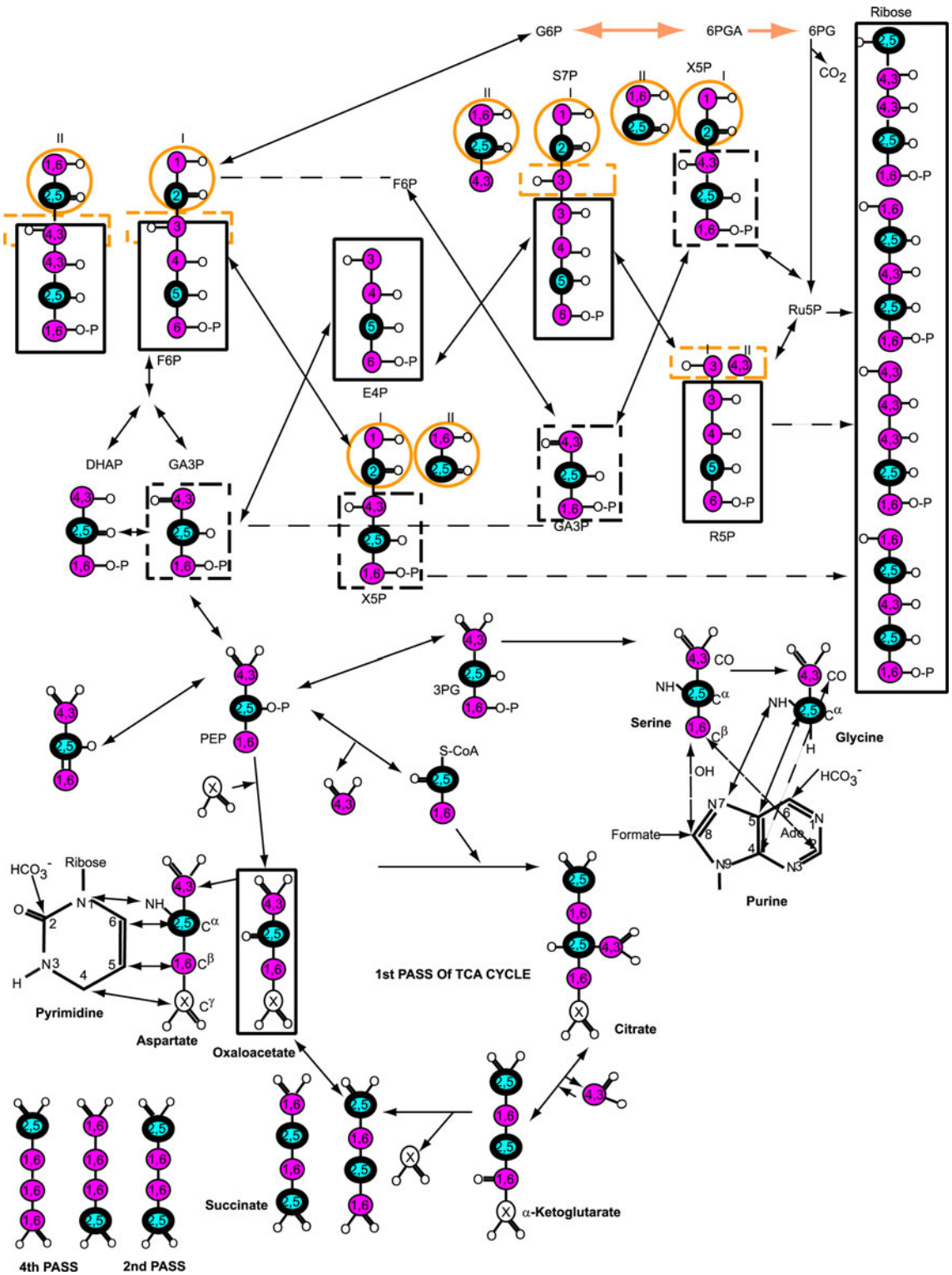

Method for growth optimization

The growth of the *E. coli* mutant strain tktA was optimized for biomass production as described previously for other strains (Thakur et al. 2010a, b). Only in this case kanamycin was added to both the growth media and the LB plates. Briefly, a single colony of tktA *E. coli* grown on kanamycin LB plates was inoculated into a 5 ml starter culture in unlabeled LMR medium and incubated at 37°C

overnight. The overnight culture was pelleted, the pellet was washed twice in 1× phosphate-buffered saline (PBS) and dissolved in fresh 5 ml LMR medium with no carbon source; 1 ml from this solution was diluted into a 50 ml culture in LMR medium, and grown overnight at 37°C. The 50 ml culture was pelleted prior to complete saturation of these cells, the pellet was washed twice in 1× PBS, and then dissolved in 50 ml of fresh medium with no carbon sources. A 5 ml aliquot of this resuspension was added to 500 ml LMR medium supplemented with labeled carbon sources (glucose) and incubated at 37°C for 6–8 h.

P1 nuclease digestion and boronate affinity column nucleotide purification

The labeled ribonucleotides were isolated from *E. coli* cultures as described previously (Batey et al. 1992; Dayie and Thakur 2010). Briefly, the mixture containing the digested nucleic acids was separated into individual ribo- or deoxyribo-nucleotides using a *cis-diol* boronate affinity chromatography column as described (Batey et al. 1992; Dayie and Thakur 2010). The purity of these rNMPs was confirmed by NMR prior to use in phosphorylation reactions. For relaxation experiments, the uniformly or site specifically labeled cytidine 5′-monophosphate (CMP) was first dissolved in 10 mM phosphate buffer pH 6.4 (made in 100% D_2O), lyophilized and re-suspended in 250 µl of 100% D8 Glycerol. The site specific labeled CMP (extracted from tktA *E. coli* strain grown on [2-^{13}C]-glucose) was first separated by FPLC, re-suspended in 10 mM phosphate buffer pH 6.4 (this buffer was again made in 100% D_2O), lyophilized, and re-dissolved in 100% D8 glycerol.

Enzymatic phosphorylation

The enzymatic phosphorylation procedure was adapted from the method developed by Nyholm et al. (1995). The individual rNMPs were chromatographically separated and purified, and the purified rNMPs were phosphorylated to the corresponding rNTPs using kinases specific for each of the rNMPs in the presence of a coupled thioredoxin-dithiothretol redox system (Nyholm et al. 1995). Labeled rAMP was converted to the labeled rATP enzymatically in less than 1 h, and the progression of the rATP phosphorylation was monitored on an analytical TARGA C18 column. This reaction mixture was purified further on a TARGA C18 column (250 × 20 mm) by reverse phase FPLC. A linear gradient of Buffer A (0.1 M KH_2PO_4) and Buffer B (20% MeCN in 0.1 M KH_2PO_4) were run at a flow rate of 10 ml/min in five column volumes for the separation. Collected ATP fractions were pooled and desalted prior to use for NMR and RNA transcription reactions.

RNA labeling and transcription

RNA samples were synthesized by in vitro transcription with T7 RNA polymerase using unlabeled rCTP, rGTP, and rUTP combined with either uniformly ^{13}C/^{15}N-labeled rATP or site specifically ^{13}C/^{15}N-labeled rATP using established protocols (Milligan et al. 1987; Milligan and Uhlenbeck 1989; Puglisi and Wyatt 1995). A second set of samples were also made using unlabeled rATP, rCTP, and rGTP, combined with either uniformly ^{13}C/^{15}N-labeled rUTP or site specifically ^{13}C/^{15}N-labeled rUTP. A mutant His-tagged T7 RNA polymerase (Guillerez et al. 2005) was overexpressesed in *E. coli* BL21 (DE3) and purified on a Ni-chelating Sepharose column (Pharmacia) using established methods. The DNA promoter sequence, or top strand, has a C nucleotide at the −18 T7 promoter region (Baklanov et al. 1996) (CTOP) with the following sequence: 5′ CTA ATA CGA CTC ACT ATA G-3′. The corresponding templates used for NMR analysis for D5 RNA and A-Site RNA were 5′-g AAC CGT ACG TGC GAC TTT CAT CGC ATA CGG CTC c TAT AGT GAG TCG TAT TAG-3′ (lower case letters represent nucleotides introduced to improve transcription yield and they do not affect the catalytic ability of the D123 ribozyme (Gumbs et al. 2006); and 5′-mGmGC GAC TTC ACC CGA AGG TGT GAC GCC TAT AGT GAG TCG TAT TAG-3′ (the lower case letter m represents 2′-methoxyl modification of the first two nucleotides of the template strand). Two terminal 2′-*O*-methyl modifications in the template strand indicated by "m" were introduced to substantially reduce the amount of transcripts with extra nucleotides at the 3′-end (Kao et al. 1999). The optimal transcription conditions were found by a systematic variation of Mg^{2+} and rNTP to be as follows: for D5 RNA these were 15 mM total NTPs and 13.7 mM Mg^{2+}, and for A-Site RNA these were 10 mM total NTPs and 15 mM Mg^{+2}. The reactions were carried out in transcription buffer C (40 mM Tris–HCl, pH 8.1, 1 mM spermidine, 5 mM dithiothreitol (DTT), 0.01% Triton X-100, 80 mg/ml PEG 8000), 300 nM each DNA strand, and 1.5 µl T7 polymerase (optimized amount) per 40 µl of transcription volume. After 3 h of incubation at 37°C, each RNA from the transcription reaction was purified and dialyzed extensively as described (Dayie 2005). After dialysis, the RNA was lyophilized, and resuspended into NMR buffer (100 mM KCl, 10 mM potassium phosphate pH 6.2, 8% D_2O (or 100%), and a trace of sodium azide) with or without 3 mM $MgCl_2$. A small sample was hydrolyzed in 1.0 M sodium hydroxide, neutralized with HCl, and the UV absorbance was used to calculate the sample concentrations. NMR sample volumes were 250 µl in Shigemi tubes, with concentrations of 0.1 mM and 0.4 mM for D5 and A-Site RNAs respectively.

NMR experiments

All NMR experiments were run on a four channel Bruker Avance III 600 MHz spectrometer equipped with a triple resonance probe with actively shielded z-axis gradient. All the experiments were conducted at temperatures from 15 to 45°C. The NMR data sets were processed and the peak positions and intensities were analyzed with Bruker's TOPSPIN 2.1 as described previously (Dayie and Thakur 2010). One dimensional (1D) ^{13}C spectra and two-dimensional non-constant-time ^{1}H, ^{13}C-heteronuclear single quantum correlation (HSQC) spectra (Bodenhausen and Ruben 1980; Bax et al. 1990) were acquired to analyze the rNMP fractions extracted from each bacterial strain. Three methods were used to ascertain the labeling pattern of carbon in both the ribose and the base rings. First, the fractional ^{13}C enrichment at each carbon site was quantified using the ^{13}C satellite of the well resolved H1′ resonance in a 1D ^{1}H experiment without ^{13}C decoupling during acquisition. The ratio of the sum of the intensities of satellite peaks to the sum of the intensities of the satellite and center peaks was used to calculate the absolute enrichment level. Second, for cases of overlap in the 1D experiments, a 2-bond ($^{2}J_{HN}$) HSQC (Dayie and Thakur 2010; Thakur et al. 2010b) was used. Here again the ratio of the sum of the intensities of satellite peaks to the sum of the intensities of the satellite and center peaks was used to calculate the absolute enrichment level. Third, for those carbon sites where no quantitative information could be obtained from either the 1D or the 2-bond ($^{2}J_{HN}$) HSQC experiments, the absolute enrichment of proton resonances obtained from the 1D ^{1}H experiments and relative enrichment values obtained from a carbon HSQC spectrum were used to compute the absolute enrichment levels (Walker et al. 1982; Kishore et al. 2005).

To ascertain the effect of constant time and band selective decoupling on spectral sensitivity, three HSQC variants were used. Non-constant time HSQC with and without band-selective decoupling during the t_1 carbon evolution period and constant-time HSQC experiments were run on uniform and site-specific ^{13}C labeled RNA samples. For the band-selective decoupled HSQC, WURST-2 decoupling of C2′ resonances was used during the carbon evolution period, as described previously for ^{13}C-edited NOESY (Brutscher et al. 2001; Dayie 2005). For constant time experiments, total constant-time delays of 26.6 and 53.2 ms were used to examine the effects of resolution and sensitivity.

To explore the effect of uniform ^{13}C labeling on relaxation measurements, longitudinal (R_1) relaxation rates were measured for ribose C1′ and cytosine nucleobase C6 carbons using TROSY detected experiments (Hansen and Al-Hashimi 2007) for uniformly and site-specifically labeled samples without the need for selective pulses. The following R_1 mixing times were used for both uniformly labeled and site specifically labeled CMPs dissolved in perdeuterated glycerol (prepared as described above): 21.1, 63.4, 147.8, 316.8, 401.3 and 823.7 ms. The experiments were carried out at 45°C using TROSY detected R_1 experiments with the carbon carrier at 142.4 ppm. For R_1 measurements on uniformly ATP-labeled D5 RNA and D5 RNA made using site specific labeled ATP, the following mixing times were used: 21.1 (2×), 63.4, 147.8, 232.3, 401.3,528.0, 612.5, and 823.7 ms. For both samples, the carbon carrier was placed at 89.9 ppm. R_1 rates were fitted assuming monoexponential decay as described (Eldho and Dayie 2007). The uncertainty, ΔR_1, was calculated based on random noise of the spectra, using the expression, $\Delta R_1 = \delta_e/I$, where δ_e is the r.m.s. noise measured in the reference spectrum, and I is the intensity of each peak (Ishima and Torchia 2005).

The magnesium ion binding surface of D5 RNA was mapped by the chemical shift perturbation method using non-constant time two-dimensional ^{1}H–^{13}C HSQC experiment. Spectra were collected on ~0.1 mM uniformly ^{13}C/^{15}N-ATP labeled or site selectively ATP labeled D5 RNA samples in either 0 or 4 mM $MgCl_2$. Each complex was heated to 363 K for 1 min and rapidly cooled on ice for 10 min before taking the NMR spectra. All the experiments were carried out at 298 K on a D5 sample in MOPS buffer pH 6.5, and 100 mM KCl. The non-constant time HSQC utilized pulsed field gradients for coherence order selection and sensitivity enhancement (Palmer et al. 1991; Kay et al. 1992), each dataset consisted of 128 complex points in t_1, 2 K real points in t_2, 128 scans per t_1 increment, and a recycle delay of 1 s. The carbon carrier was placed at 89 ppm and a spectral width of 8 ppm was used. All the data sets were processed identically without applying any window functions. Similarly, binding of paramomycin to ~0.4 mM uniformly ^{13}C/^{15}N-ATP labeled or site selectively ATP labeled A-Site RNA fragment was monitored through changes in the peak positions of each nucleotide. Experiments were conducted at 315 K in 10 mM potassium phosphate buffer (pH 6.5), and 100 mM KCl. For each experiment a spectral width of 8 ppm, a 1.3 s recycle delay and 256 scans were used.

Results

Alternate site-specifically labeled rNMP from biomass production using mutant tktA E. coli

To test the hypothesis that tktA *E. coli* will shunt most of the metabolic flux through the oPPP and suppress scrambling of labels in the ribose ring, the growth of both wild

type *E. coli* strain K12 and mutant tktA *E. coli* on [2-^{13}C]-glucose were compared (Fig. 1). The level of ^{13}C labeling efficiency was estimated using three methods of 1D ^{1}H or natural abundance ^{13}C carbon spectra, long range proton-nitrogen correlations in ^{15}N-HSQC spectra as described previously (Dayie and Thakur 2010; Thakur et al. 2010b) or the method of fractional enrichment (Walker et al. 1982; Kishore et al. 2005).

For wild type K12, from the 1D ^{1}H spectrum of AMP, the C1′ ribose carbon was significantly enriched, as its attached proton displayed satellite peaks due to the ^{13}C–^{1}H coupling (^{1}J = 168.9 Hz). The intensity ratio of the center peak to the sum of its two satellite peaks was 5.71:20.06, indicating that C1′ was approximately 77% enriched. A similar consideration for tktA *E. coli* indicates that the label at C1′ was ~93% enriched (Fig. 2). Obtaining the enrichment level for the other ribose carbons other than C1′ was problematic using the 1D method because of extensive overlap. To obtain the enrichment levels for these ribose carbon atoms, a 2D ^{13}C-HSQC experiment was conducted. The results are summarized in Table 1 where the relative intensity of each cross-peak is expressed as the percentage of the intensity of the C1′ cross-peak.

Using the absolute enrichment of C1′ carbon, the relative enrichment obtained from either 1D direct carbon or 2D HSQC experiments was used to find the absolute enrichment level. For instance for wild type K12, the ^{13}C content of C2′ and C4′ were found to be approximately 38.4 and 46.9% respectively of C1′. Given that C1′ was 77% enriched, we deduced that C2′ and C4′ were enriched 29 and 36% respectively, as summarized in Fig. 2 and Table 1. In contrast, for tktA *E. coli* the label at C2′ was ~7% and the label at C4′ was ~19% (Fig. 2).

Growth of mutant tktA *E. coli* on [1-^{13}C]-glucose led to maximum labeling at the C5′ position (~87%), ~20% labeling at the C1′ and essentially no labeling (<2%) elsewhere in the ribose ring (Fig. 3A, B). Furthermore, growth of mutant tktA *E. coli* on a mixture of [1-^{13}C]-glucose and [2-^{13}C]-glucose led to maximum labeling at the C1′ position (~54%), high labeling at the C5′ (~35%), some labeling at C2′ and C4′, and very little label (<1%) at C3′ in the ribose ring (Fig. 3C, D).

Selective labeling removes unwanted couplings without compromising sensitivity

As shown previously when the ribose ring is uniformly labeled, the ribose C2′ and C4′ positions form a triplet and the C1′ and C5′ positions form doublets in non-constant time HSQC spectra (Dayie and Thakur 2010). These unwanted splittings can be removed using either constant time experiments (Bax et al. 1979; Bax and Freeman 1981; Vuister and Bax 1992; Van de Ven and Philippens 1992),

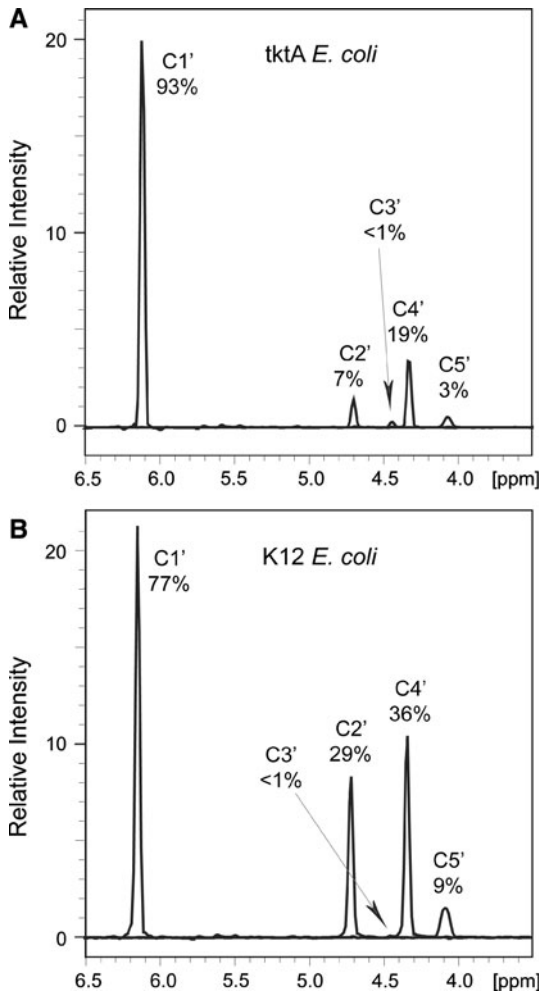

Fig. 2 1D ^{1}H traces extracted from 2D ^{1}H-^{13}C non-constant HSQC spectra for each carbon position within the ribose ring (C1′, C2′, C3′, C4′, and C5′) of rAMP showing the ^{13}C isotopic enrichment levels in two *E. coli* variants grown on [2-^{13}C]-glucose. The percentage labels were calculated as described in the text. **A** Labeling pattern found in the ribose region of rAMP isolated from tktA *E. coli* strain grown with [2-^{13}C]-glucose. **B** Labeling pattern found in the ribose region of rAMP isolated from K12 *E. coli* strain grown with [2-^{13}C]-glucose

adiabatic band selective decoupling schemes (Kupce and Wagner 1996; Brutscher et al. 2001;Dayie 2005), or maximum entropy reconstruction-deconstruction (Shimba et al. 2003).

Unfortunately, the length of the constant time period (T) limits the acquisition times (t_1^{max}) to multiples of the homonuclear coupling constant (J_{CC}), i.e. $t_1^{max} = n/J_{CC}$ where n is an integer, $J_{C5C6} = 67$ Hz and $J_{C1'C2'} = 43$ Hz. To obtain reasonable digital resolution, large values of T are needed. Also during the constant-time period (T), the decay of the transverse magnetization is proportional to exp ($-R_2T$), where R_2 is the homogenous transverse rate constant. The long constant-time delays needed to improve resolution lead to significant signal attenuation for RNA molecules larger than 30 nucleotides (Dayie 2005), and

Table 1 ^{13}C enrichment levels at various carbon positions within ribonucleotides harvested from tkta *E. coli* grown on [1-^{13}C]-glucose, [2-^{13}C]-glucose, and an equimolar mixture of [1-^{13}C]-glucose and [2-^{13}C]-glucose

Carbon position labeled	^{13}C-Carbon source: 1-glucose	^{13}C-Carbon source: 2-glucose	^{13}C-Carbon source: 1-glucose and 2-glucose
Purine[a]			
Ade C2	75 ± 1	11 ± 1	47 ± 2
C8	44 ± 1	2 ± 1	21 ± 2
Pyrimidine[a]			
C5	43 ± 4	28 ± 4	34 ± 1
C6	28 ± 1	28 ± 4	26 ± 1
Ribose			
C1′[a]	20 ± 4	93 ± 2	54 ± 2
C2′[b]	<2	7 ± 1	8 ± 1
C3′[b]	<2	<1	<1
C4′[b]	<2	19 ± 1	14 ± 1
C5′[c]	87 ± 12	<3	35 ± 1

[a] The percentage label is calculated as an average of two methods: (1) the ratio of the sum of the intensities of satellite peaks to the sum of the intensities of the satellite and center peaks using the 2-bond ^{15}N HSQC without ^{13}C decoupling during acquisition and (2) the ratio of the sum of the intensities of satellite peaks to the sum of the intensities of the satellite and center peaks using the 1D ^{1}H experiment without ^{13}C decoupling during acquisition as described in the text

[b,c] The percentage label (Plabel) is calculated as in (a) but this time with only method (2)

thus a compromise must be found between sensitivity (small values of T) and resolution (large values of T) when using uniformly labeled samples. With the selective labels, one is not forced to compromise resolution for improved sensitivity or vice versa (Fig. 4). To obtain the spectral resolution achievable using selective labels, a constant time delay of T = 53.2 ms is needed. Yet under these conditions, most of the useful signals are lost due to rapid signal decay (Fig. 4). When resolution is not an issue, a constant time delay of T = 26.6 ms is adequate to obtain good signal-to-noise ratio.

Selective labeling allows facile monitoring of the response of the catalytic lynchpin D5 RNA to magnesium ion binding

To demonstrate the usefulness of the site selectively labeled nucleotides for mapping binding interactions, the 36-nt D5 RNA element (Dayie and Padgett 2008; Toor et al. 2008) was transcribed using either uniformly ^{13}C/^{15}N-labeled ATP or site selectively-labeled ATP derived from tktA *E. coli* cells grown on [2-^{13}C]-glucose as described above. Three structural elements implicated in the catalytic activity of the ribozyme (Boulanger et al. 1995; Peebles et al. 1995; Schmidt et al. 1996; Dayie and Padgett 2008; Toor et al. 2008) are critical Mg^{2+} ions binding sites: the highly conserved trinucleotide AGC sequence, a variable two nucleotide AA asymmetrical bulge and a capping GAAA tetraloop (Chanfreau and Jacquier 1994; Abramovitz et al. 1996; Zhang and Doudna 2002; Seetharaman et al. 2006; Toor et al. 2008). These crucial bulge and internal loop nucleotides (A17, A24, A28) have much more reduced intensity in a uniformly labeled sample than in the site-selective labeled sample (Fig. 5A, B), and as expected these nucleotides are responsive to the presence of magnesium ions (Seetharaman et al. 2006). The selective labels reduce the overlap within the ribose C1′ region that can be very crowded and enable the facile monitoring of key nucleotides involved in magnesium ion binding without the need for band selective decoupling or constant-time evolution NMR experiments (Brutscher et al. 2001; Dayie 2005).

Site selective labeling affords more accurate relaxation rate measurements using non-constant time non-selective pulse experiments

As a fourth demonstration of the usefulness of the site selectively versus the uniformly labeled nucleotides for quantifying dynamics in RNA, TROSY detected R_1 experiments were carried out on a number of samples. The highly conserved 36-nt D5 RNA was transcribed using either uniformly ^{13}C/^{15}N-labeled ATP or site selectively-labeled ATP derived from tktA *E. coli* cells grown on [2-^{13}C]-glucose.

For R_1 measurements, adjacent carbons can contribute significantly to the relaxation of macromolecules, and so we expect the selective labels to make a significant difference in the accuracy of the measured rates. As is readily apparent from Fig. 6, there is a discrepancy between R_1 measured for uniformly and site-selectively labeled RNAs: for the 36 nt D5 RNA the discrepancy for the C1′ carbon is not only 0.54 s^{-1} (2.2 ± 0.07 s^{-1} for selective labeling versus 1.6 ± 0.31 s^{-1} for uniform labeling) but also the fit to a monoexponential decay function is only applicable to the site selectively labeled RNA sample (Fig. 6A, B). Again, for the CMP dissolved in glycerol to mimic high molecular weight RNA, the discrepancy for the C6 carbon is ~0.2 s^{-1} (2.9 ± 0.1 s^{-1} for selective labeling versus 3.1 ± 0.3 s^{-1} for uniform labeling) and the monoexponential fit for the uniformly labeled CMP is poorer (Fig. 6C, D).

Discussion

The development of uniform isotopic labeling methods for transcribing labeled RNA (Batey et al. 1992; Nikonowicz

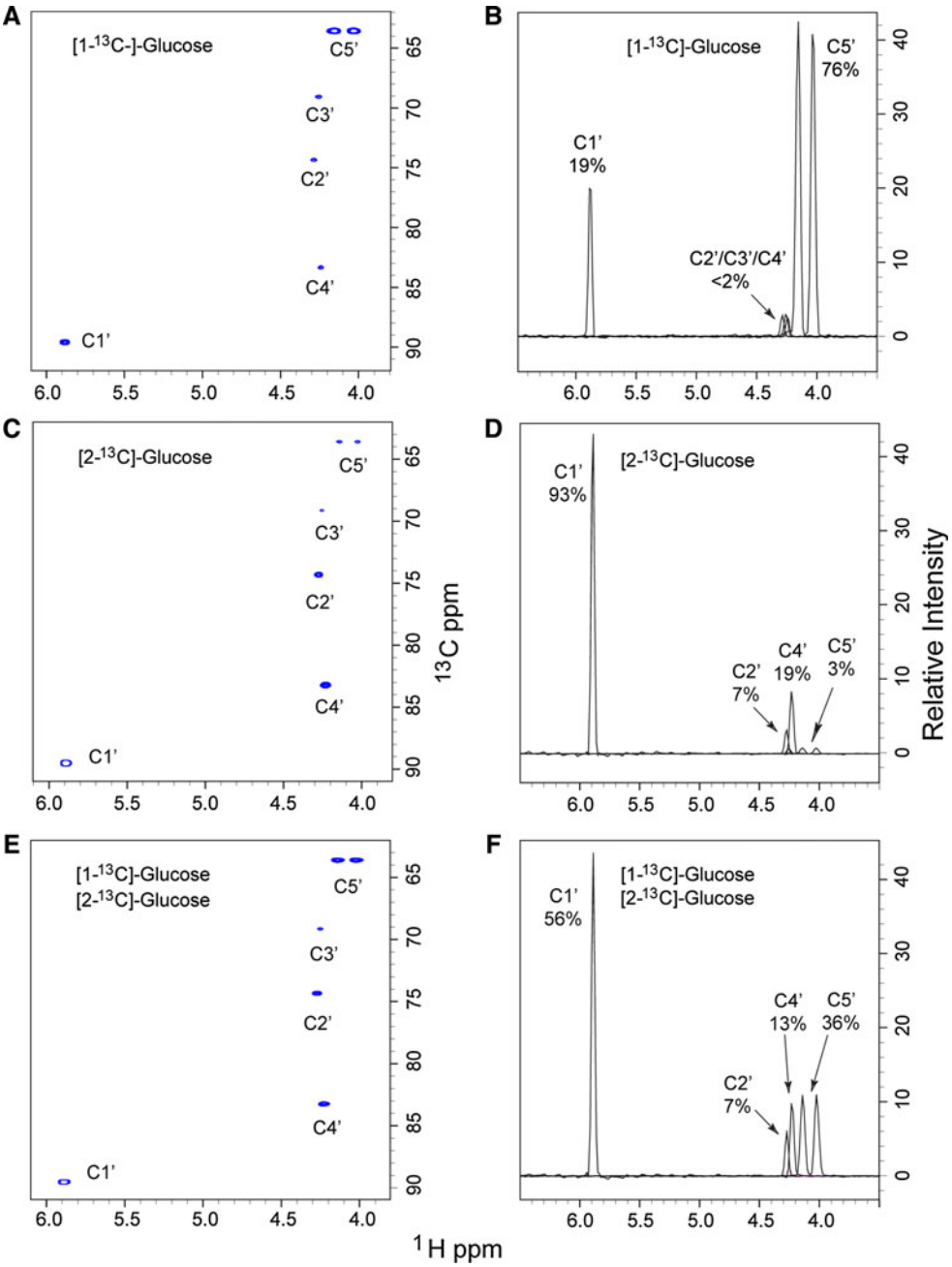

Fig. 3 The 2D ^{1}H-^{13}C non-constant HSQC spectra and the corresponding 1D ^{1}H traces extracted from the 2D spectra for each carbon position within the ribose ring (C1′, C2′, C3′, C4′, and C5′) of rCMP showing the distribution of ^{13}C isotopic enrichment levels of rCMP derived from tktA *E. coli* grown on three different carbon sources. **A**, **B** [1-^{13}C]-glucose, **C**, **D** [2-^{13}C]-glucose, and **E**, **F** mixture of [1-^{13}C]-glucose and [2-^{13}C]-glucose

et al. 1992; Michnicka et al. 1993; Hines et al. 1994) spurred the development of new solution NMR tools that enabled the structural characterization of small to medium sized RNA molecules (Batey et al. 1995; Puglisi and Wyatt 1995; Latham et al. 2005). Nonetheless, uniform labeling does not alleviate the degeneracy problem for large RNAs and it introduces direct one-bond and residual dipolar couplings that negatively impact accurate measurement of ^{13}C relaxation rates (Dayie and Thakur 2010; Thakur et al. 2010b). We set out to test the hypothesis that tktA *E. coli* strain will redirect most of the metabolic flux through the oxidative pentose phosphate pathway, limiting dilution of label within the ribose ring. This redirection of the metabolic flux would thereby afford site specific labeling within the ribose ring for useful NMR applications that overcome some of the drawbacks of uniform labeling.

Incorporation of ^{13}C into ribose ring and nucleobase of nucleotides using glucose

Within the context of metabolic pathways in *E. coli* for nucleotide metabolism (Nelson and Cox 2008; Voet et al. 2008), the ribose moiety, derived exclusively from ribose-5-phosphate (R5P), can be produced directly from glucose

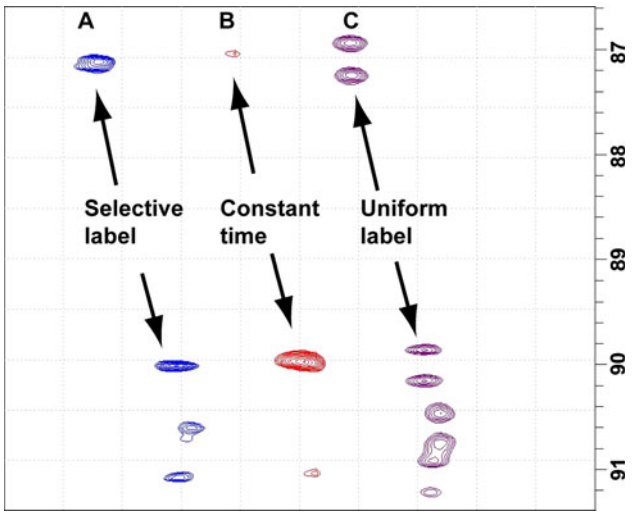

Fig. 4 NMR spectra of paromomycin bound A-Site RNA showing enhanced sensitivity and resolution afforded by site selective labeling. The experiments were performed on the RNA **A** site-selectively ^{13}C-labeled using 2D non-constant time HSQC spectra, **B** uniformly ^{13}C-labeled using 2D constant time HSQC spectra with total delay of 53.2 ms, **C** uniformly ^{13}C-labeled using 2D non-constant time HSQC spectra

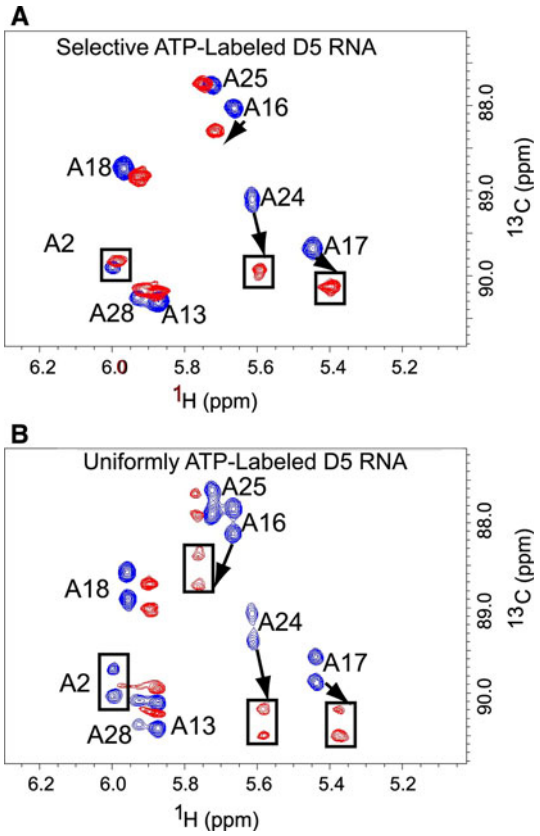

Fig. 5 NMR spectra showing enhanced resolution afforded by site selective labeling that enables facile monitoring of chemical shift perturbations of D5 RNA on binding $MgCl_2$. *Arrows* depict residues with the most chemical shift perturbation with increased magnesium ion concentration (0 and 5 mM), indicative of likely ion binding site. **A** Selective-ATP labeled D5 RNA, **B** uniform-ATP labeled D5 RNA, with both RNAs at 0.1 mM and 5 mM Mg^{2+}

or indirectly from gluconeogenic carbon sources. In the case of glucose, R5P can be produced from glucose-6-phosphate (G6P) by the elimination of the C-1 carbon from glucose as CO_2 (Fig. 1). The isotopic enrichment pattern that stems from the input glucose carbons 2–6 can be readily predicted because of the one-to-one correspondence with the label incorporation at the five ribose carbon atoms numbered 1′–5′ using the oPPP. The noPPP leads to scrambling of labels relative to the input G6P (Fig. 1). This analysis accords with the results obtained for wild type K12 *E. coli*, wherein the flux through both the oxidative and non-oxidative pathways are operative (Fig. 2). Under noPPP conditions, the five-carbon sugars (including R5P) can be recycled into three- and six-carbon glycolytic intermediates through the action of tktA and transaldolase (TAL) (Fig. 2). Thus, knocking out tktA appears to block the noPPP scrambling and retain labeling via oPPP. Our result with ~93% label at C1′ for the tktA mutant compared to ~77% for the wild type K12, both grown on [2-^{13}C]-glucose, suggests that most of the flux is indeed routed through the oPPP; however, the residual labeling of ~7% at the C2′ and 19% at C4′ positions suggests that the blockage is not complete. Rather, some of this labeling likely originates from residual tktA activity or reverse glycoslysis or both (Josephson and Fraenkel 1974).

Labeling in the nucleobases can be broadly divided into two categories based on metabolic precursors originating from glycolysis products, just as amino acid side chains can be grouped into three classes (Lundström et al. 2007). For example, G6P, isomerized to fructose-6-phosphate (F6P) and phosphorylated to fructose-6-bisphosphate (FBP), can be converted into dihydroxy acetone phosphate (DHAP) and glyceraldehyde-3-phosphate (GA3P). The rapid equilibration of DHAP and GA3P by triosephosphate isomerase (TIM) ensures that the carbonyl carbon (C-1) of GA3P is derived from glucose carbons 3 or 4, the C-2 of GA3P is derived from glucose C2 or C5, and the C-3 is derived from glucose C1 or C6 (Fig. 1). The net effect of this equilibration is that the purine nucleobase intermediates derived from serine and glycine can be enriched to ~50%. We classify these purine nucleobases into group I (adenine and guanine) and the pyrimidine nucleotides into group II (derived from OA and therefore aspartic acid). Before the entry into the TCA cycle, these group II nucleobases can also be enriched up to ~50%, but subsequent passage through the TCA cycle will reduce this further. In agreement with this analysis, we find that these group II nucleobases derived from [1-^{13}C]-glucose or a mixture of [1-^{13}C]-glucose and [2-^{13}C]-glucose gave rise to ~26–28% enrichment at the pyrimidine C6 position (Table 1).

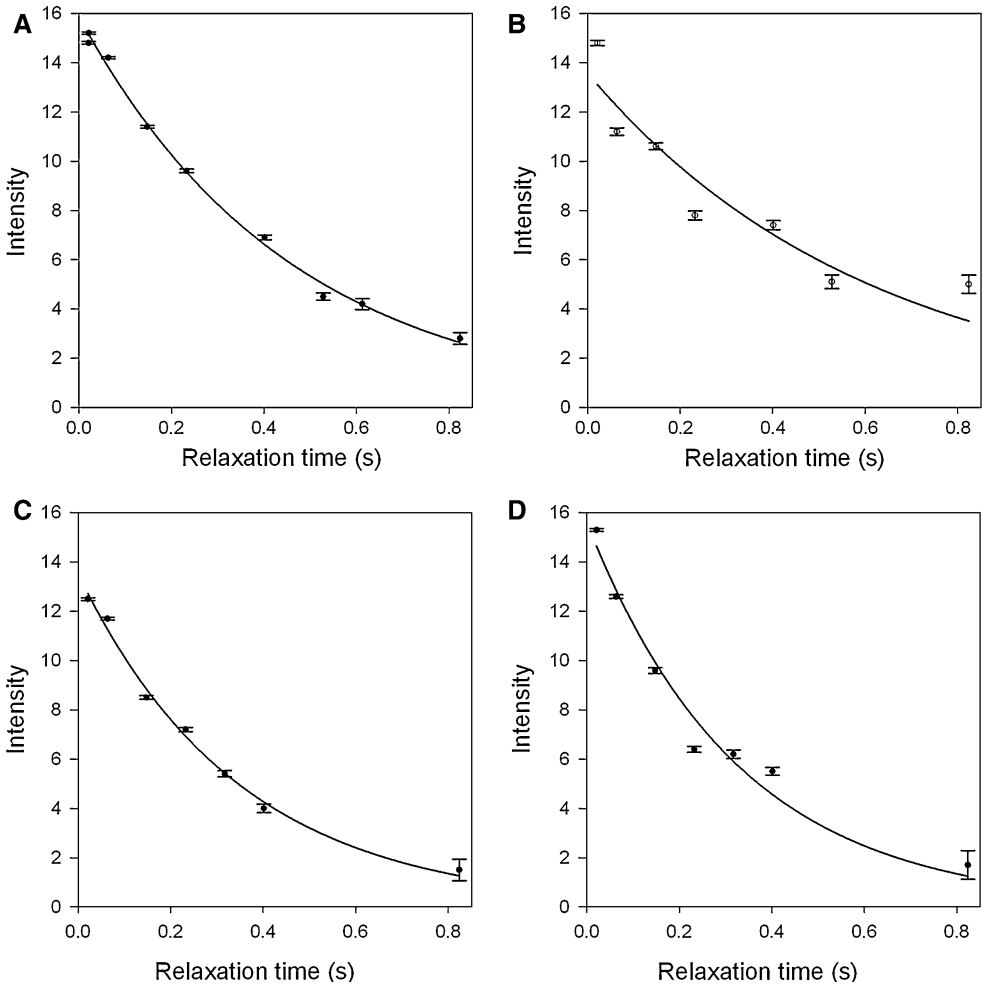

Fig. 6 Representative longitudinal R_1 relaxation decay curves for RNA samples showing marked deviation from monoexponential decay for uniformly labeled samples. **A** Ribose C1′ R_1 relaxation measurements at 25°C for the D5 RNA labeled with site selectively-labeled ATP. **B** Ribose C1′ R_1 relaxation measurements at 25°C for D5 RNA labeled with uniformly $^{13}C/^{15}N$-labeled ATP. **C** Base C6 R_1 measurements at 45°C for site specifically labeled CMP dissolved in perdeuterated glycerol to mimic ~40–50-nt RNA. **D** Base C6 R_1 measurements at 45°C for uniformly labeled CMP dissolved in perdeuterated glycerol to mimic ~40–50-nt RNA

The main advantage of using the tktA *E. coli* strain grown on glucose is that it affords the highest level of enrichment at the C1′ position using [2-^{13}C]-glucose without introducing unwanted ^{13}C1′-^{13}C2′ couplings. It also affords high level of enrichment at the C5′ position using [1-^{13}C]-glucose without any unwanted ^{13}C4′-^{13}C5′ coupling. Three different *E. coli* strains have been used in the past for alternate site specific ^{13}C isotopic labeling (Johnson et al. 2006; Johnson and Hoogstraten 2008; Dayie and Thakur 2010; Thakur et al. 2010b) using gluconeogenic carbon precursors such as glycerol that attain at most 55% enrichment in the C1′ position. Growth of wild type *E. coli* on glucose, on one hand, afforded at most 73% labeling. On the other hand, growth on acetate afforded close to 90% uniform labeling but with multiplet splitting from C2′ and C4′ (Hoffman and Holland 1995; Kishore et al. 2005). In the nucleobases, however, use of [2-^{13}C]-glucose leads to a maximum of 50% enrichment compared to ~90% attainable using [2-^{13}C]-glycerol (Johnson et al. 2006; Johnson and Hoogstraten 2008; Dayie and Thakur 2010; Thakur et al. 2010b). Also use of [1-^{13}C]-glucose again leads to a maximum of 50% enrichment in the nucleobases compared to ~90% attainable using [1,3-^{13}C]-glycerol; however since the price of [1,3-^{13}C]-glycerol is ~4× that of [1-^{13}C]-glucose, glucose is an excellent alternative in this case.

Site specific labeling of the ribose ring and purine and pyrimidine bases will advance the quantitative analysis of NMR relaxation parameters for RNA. For example, previous ^{13}C relaxation studies using uniformly labeled samples precluded the clean extraction of relaxation rates of base C5 and C6 positions in pyrimidine ring and ribose ring atoms.

Conclusion

Here we have shown that an *E. coli* strain deficient in the transketolase gene (tktA) shunts most of the metabolic flux via the oxidative pentose phosphate pathway, and as a result growth of this *E. coli* strain on a number of glucose sources affords very high levels of enrichment of nucleotides specifically labeled at C1′ and C5′ positions without the attendant deleterious one bond ^{13}C-^{13}C scalar and dipolar couplings that normally interfere with measuring accurate spin-relaxation parameters and that normally

exacerbate spectral crowding. We demonstrated the utility of this labeling approach on a 36-nt D5 RNA, wherein these specifically labeled rNTPs eliminated the extensive ^{13}C–^{13}C coupling within the nitrogenous base and ribose ring, leading to simpler and higher resolution NMR spectra. Having uncluttered spectra enabled the facile identification of nucleotides within the binding interface of the D5-Mg^{2+} complex. Finally, we showed that these selective labels enabled more accurate TROSY detected R_1 relaxation rate measurements. These selective labels should prove valuable in applying high resolution NMR analysis to RNAs that require conformational switching for their biological functions.

Acknowledgments This work was supported in part by the University of Maryland Nano-Biotechnology Award and the National Institutes of Health grant GM077326 to T.K.D. Gopal Narang for K12 culture in labeled glucose as the carbon source.

References

Abramovitz DL, Friedman RA, Pyle AM (1996) Catalytic role of 2′-hydroxyl groups within a group II intron active site. Science 271:1410–1413

Al-Hashimi HM, Walter NG (2008) RNA dynamics: it is about time. Curr Opin Struct Biol 18:321–329

Baklanov MM, Golikova LN, Malygin EG (1996) Effect on DNA transcription of nucleotide sequences upstream to T7 promoter. Nucleic Acid Res 24:3659–3660

Batey RT, Inada M, Kujawinski E, Puglisi JD, Williamson JR (1992) Preparation of isotopically labeled ribonucleotides for multidimensional NMR spectroscopy of RNA. Nucleic Acids Res 20:4515–4523

Batey RT, Battiste JL, Williamson JR (1995) Preparation of isotopically enriched RNAs for heteronuclear NMR. Methods Enzymol 261:300–322

Bax A, Freeman R (1981) Investigation of complex networks of spin–spin coupling by two-dimensional NMR. J Magn Reson 44:542–561

Bax A, Mehlkopf AF, Smidt J (1979) Homonuclear broad-band decoupled absorption spectra. J Magn Reson 35:167–169

Bax A, Ikura M, Kay LE, Torchia DA, Tschudin R (1990) Comparison of different modes of two-dimensional reverse correlation NMR for the study of proteins. J Magn Reson 86:304–318

Bodenhausen G, Ruben DJ (1980) Natural abundance nitrogen-15 NMR by enhanced heteronuclear spectroscopy. Chem Phys Lett 69:185–189

Boulanger SC, Belcher SM, Schmidt U, Dib-Hajj SD, Schmidt T, Perlman PS (1995) Studies of point mutants define three essential paired nucleotides in the domain 5 substructure of a group II intron. Mol Cell Biol 15:4479–4488

Brutscher B, Boisbouvier J, Kupce E, Tisne C, Dardel F, Marion D, Simorre JP (2001) Base-type-selective high-resolution ^{13}C edited NOESY for sequential assignment of large RNAs. J Biomol NMR 19:141–151

Chanfreau G, Jacquier A (1994) Catalytic site components common to both splicing steps of a group II intron. Science 266: 1383–1387

Clowes R (1968) In: Hayes W (ed) Experiments in microbial genetics. Wiley, New York

Covert MW, Palsson BO (2002) Transcriptional regulation in constraints-based metabolic models of *Escherichia coli*. J Biol Chem 277:28058–28064

Dayie KT (2005) Resolution enhanced homonuclear carbon decoupled triple resonance experiments for unambiguous RNA structural characterization. J Biomol NMR 32:129–139

Dayie KT (2008) Key labeling technologies to tackle sizeable problems in RNA structural biology. Int J Mol Sci 9:1214–1240

Dayie KT, Padgett RA (2008) A glimpse into the active site of a group II intron and maybe the spliceosome, too. RNA 14: 1697–1703

Dayie TK, Thakur CS (2010) Site-specific labeling of nucleotides for making RNA for high resolution NMR studies using an *E. coli* strain disabled in the oxidative pentose phosphate pathway. J Biomol NMR 47:19–31

Eldho NV, Dayie KT (2007) Internal bulge and tetraloop of the catalytic domain 5 of a Group II intron ribozyme are flexible: implications for catalysis. J Mol Biol 365:930–944

Guillerez J, Lopez PJ, Proux F, Launay H, Dreyfus M (2005) A mutation in T7 RNA polymerase that facilitates promoter clearance. Proc Natl Acad Sci U S A 102:5958–5963

Gumbs OH, Padgett RA, Dayie KT (2006) Fluorescence and solution NMR study of the active site of a 160-kDa group II intron ribozyme. RNA 12:1693–1707

Hall KB (2008) RNA in motion. Curr Opin Chem Biol 12:612–618

Hansen AL, Al-Hashimi HM (2007) Dynamics of large elongated RNA by NMR carbon relaxation. J Am Chem Soc 129:16072–16082

Hines JV, Landry SM, Varani G, Tinoco I (1994) Carbon-proton scalar couplings in RNA—3D heteronuclear and 2D isotope-edited NMR of A C-13 labeled extra-stable hairpin. J Am Chem Soc 116:5823–5831

Hoffman DW, Holland JA (1995) Preparation of C-13-labeled ribonucleotides using acetate as an isotope source. Nucleic Acids Res 23:3361–3362

Ishima R, Torchia DA (2005) Error estimation and global fitting in transverse-relaxation dispersion experiments to determine chemical-exchange parameters. J Biomol NMR 32:41–54

Johnson JE Jr, Hoogstraten CG (2008) Extensive backbone dynamics in the GCAA RNA tetraloop analyzed using ^{13}C NMR spin relaxation and specific isotope labeling. J Am Chem Soc 130:16757–16769

Johnson JE, Julien KR, Hoogstraten CG (2006) Alternate-site isotopic labeling of ribonucleotides for NMR studies of ribose conformational dynamics in RNA. J Biomol NMR 35:261–274

Josephson BL, Fraenkel DG (1969) Transketolase mutants of *Escherichia coli*. J Bacteriol 100:1289–1295

Josephson BL, Fraenkel DG (1974) Sugar metabolism in transketolase mutants of *Escherichia coli*. J Bacteriol 118:1082–1089

Kao C, Zheng M, Rüdisser S (1999) A simple and efficient method to reduce non templated nucleotide addition at the 3 terminus of RNAs transcribed by T7 RNA polymerase. RNA 5:1268–1272

Kay LE, Keifer P, Saarinen T (1992) Pure absorption gradient enhanced heteronuclear single quantum correlation spectroscopy with improved sensitivity. J Am Chem Soc 114:10663–10665

Kishore AI, Mayer, Prestegard JH (2005) Partial 13C isotopic enrichment of nucleoside monophosphates: useful reporters for NMR structural studies. Nucleic Acids Res 33:e164

Kupce E, Wagner G (1996) Multisite band-selective decoupling in proteins. J Magn Reson B 110:309–312

Latham MR, Brown DJ, McCallum SA, Pardi A (2005) NMR methods for studying the structure and dynamics of RNA. Chembiochem 6:1492–1505

Lu K, Miyazaki Y, Summers MF (2010) Isotope labeling strategies for NMR studies of RNA. J Biomol NMR 46:113–125

Lundström P, Teilum K, Carstensen T, Bezsonova I, Wiesner S, Hansen DF, Religa TL, Akke M, Kay LE (2007) Fractional 13C enrichment of isolated carbons using [1-13C]- or [2-13C]-glucose facilitates the accurate measurement of dynamics at backbone Calpha and side-chain methyl positions in proteins. J Biomol NMR 38:199–212

Michnicka MJ, Harper JW, King GC (1993) Selective isotopic enrichment of synthetic RNA: application to the HIV-1 TAR element. Biochemistry 32:395–400

Milligan JF, Uhlenbeck OC (1989) Synthesis of small RNAs using T7 RNA polymerase. Methods Enzymol 180:51–62

Milligan JF, Groebe DR, Witherell GW, Uhlenbeck OC (1987) Oligoribonucleotide synthesis using T7 RNA polymerase and synthetic DNA templates. Nucleic Acid Res 15:8783–8798

Nelson DL, Cox MM (2008) Lehninger principles of biochemistry. W.H. Freeman, New York

Nikonowicz EP, Sirr A, Legault P, Jucker FM, Baer LM, Pardi A (1992) Preparation of ^{13}C and ^{15}N labelled RNAs for heteronuclear multi-dimensional NMR studies. Nucleic Acids Res 20:4507–4513

Nyholm T, Andang M, Hotchkiss G, Hard T, Baumann H, Larsson S, Ahrlund-Richter L (1995) A method for production of $^{13}C/^{15}N$ double labelled RNA in *E. coli*, and subsequent in vitro synthesis of ribonucleotide 5′ triphosphates. J Biochem Biophys Methods 30:59–68

Palmer AG, Cavanagh J, Wright PE, Rance M (1991) Sensitivity improvement in proton-detected two-dimensional heteronuclear correlation NMR spectroscopy. J Magn Reson 93:151–170

Peebles CL, Zhang M, Perlman PS, Franzen JS (1995) Catalytically critical nucleotide in domain 5 of a group II intron. Proc Natl Acad Sci U S A 92:4422–4426

Puglisi JD, Wyatt JR (1995) Biochemical and NMR studies of RNA conformation with an emphasis on RNA pseudoknots. Methods Enzymol 261:323–350

Sambrook J, Russell DW (2001) Molecular cloning: a laboratory manual. Cold Spring Harbor Laboratory, Cold Spring Harbor, NY

Schmidt U, Podar M, Stahl U, Perlman PS (1996) Mutations of the two-nucleotide bulge of D5 of a group II intron block splicing in vitro and in vivo: phenotypes and suppressor mutations. RNA 2:1161–1172

Schultheisz HL, Szymczyna BR, Scott LG, Williamson JR (2008) Pathway engineered enzymatic de novo purine nucleotide synthesis. ACS Chem Biol 3:499–511

Seetharaman M, Eldho NV, Padgett RA, Dayie KT (2006) Structure of a self-splicing group II intron catalytic effector domain 5: parallels with spliceosomal U6 RNA. RNA 12:235–247

Shimba N, Stern AS, Craik CS, Hoch JC, Dotsch V (2003) Elimination of 13Cα splitting in protein NMR spectra by deconvolution with maximum entropy reconstruction. J Am Chem Soc 125:2382–2383

Soupene E, van Heeswijk WC, Plumbridge J, Stewart V, Bertenthal D, Lee H, Prasad G, Paliy O, Charernnoppakul P, Kustu S (2003) Physiological studies of *Escherichia coli* strain MG1655: growth defects and apparent cross-regulation of gene expression. J Bacteriol 185:5611–5626

Thakur CS, Dayie TK (2011) Asymmetry of (13)C labeled 3-pyruvate affords improved site specific labeling of RNA for NMR spectroscopy. J Biomol NMR. doi:10.1007/s10858-011-9581-6

Thakur CS, Brown ME, Sama JN, Jackson ME, Dayie TK (2010a) Growth of wildtype and mutant *E. coli* strains in minimal media for optimal production of nucleic acids for preparing labeled nucleotides. Appl Microbiol Biotechnol 88:771–779

Thakur CS, Sama JN, Jackson ME, Chen B, Dayie TK (2010b) Selective ^{13}C labeling of nucleotides for large RNA NMR spectroscopy using an *E. coli* strain disabled in the TCA cycle. J Biomol NMR 48:179–192

Toor N, Keating KS, Taylor SD, Pyle AM (2008) Crystal structure of a self-spliced group II intron. Science 320:77–82

Van de Ven FJM, Philippens MEP (1992) Optimization of constant-time evolution in multidimensional experiments. J Magn Reson 97:637–644

Voet D, Voet JG, Pratt CW (2008) Fundamentals of biochemistry, 3rd edn. Wiley, New York

Vuister GW, Bax A (1992) Resolution enhancement and spectral editing of uniformly 13C enriched proteins by homonuclear broadband 13C–13C decoupling. J Magn Reson 98:428–435

Walker TE, Han CH, Kollman VH, London RE, Matwiyof NA (1982) ^{13}C nuclear magnetic resonance studies of the biosynthesis by *Microbacterium ammoniaphilum* of L-glutamate selectively enriched with carbon-13. J Biol Chem 257:1189–1195

Zhang L, Doudna JA (2002) Structural insights into group II intron catalysis and branch-site selection. Science 295:2084–2088